JOURNAL OF GEOPHYSICAL RESEARCH, VOL. 98, NO. E9, PAGES 17,049–17,060, SEPTEMBER 25, 1993

Compressional Tectonism on Mars

THOMAS R. WATTERS

Center for Earth and Planetary Studies, National Air and Space Museum, Smithsonian Institution, Washington, D.C.

Contractional features on Mars were identified on the basis of photogeologic evidence of crustal shortening and comparison with terrestrial and planetary analogs. Three classes of structures, wrinkle ridges, lobate scarps and high-relief ridges, were mapped and their spatial and temporal distribution assessed. Wrinkle ridges account for over 80% of the total cumulative length of the mapped contractional features and occur in smooth plains material interpreted to be volcanic in origin. Lobate scarps, not wrinkle ridges, are the dominant contractional feature in Martian highland material. The pattern of contractional features in the western hemisphere reflects the hemispheric-scale influence of the Tharsis rise. Although no comparable hemispheric-scale pattern is observed in the eastern hemisphere, prominent regional-scale patterns exist, the most notable of which occurs in Hesperia Planum. Contractional features that locally parallel the trend of the crustal dichotomy boundary in the eastern hemisphere suggest the influence of stresses related to the evolution of the dichotomy. Compressional deformation apparently peaked during the Early Hesperia, if the tectonic features are roughly the same age as the units in which they occur. This peak in compressional deformation corresponds with Early Hesperian volcanic resurfacing of a large portion of the planet. Thermal history models for Mars, based on an initially hot planet, are inconsistent with estimates of the timing of peak compressional tectonism and the rate of volcanism. A pulse of global volcanism during the Early Hesperian may have resulted in a punctuated episode of rapid cooling and global contraction that contributed to compressional tectonism. Although global contraction may have contributed a significant component of the total stress that resulted in compressional deformation on Mars, nonhydrostatic horizontal stresses derived from local and regional-scale sources are necessary to account for the uniform orientations of the tectonic features.

INTRODUCTION

Landforms attributed to compressional deformation are abundant on Mars. Systems of contractional features occur on the local, regional, and even hemispheric scale. Previous efforts to survey contractional features on Mars have centered on mapping landforms that can be broadly classified as ridges. The first such survey using Viking Orbiter images was made by *Chicarro et al.* [1985]. They mapped thousands of ridges over many units with widely different ages. However, because wrinkle ridges, generally thought to be contractional in origin, are grouped with landforms probably best described as plain or simple ridges, the origin of a large percentage of the mapped features may not be tectonic. Another view of the global distribution of ridges can be obtained from the 1:15 million-scale geologic maps [*Scott and Tanaka*, 1986; *Greeley and Guest*, 1987; *Tanaka and Scott*, 1987]. However, in many cases, these maps only indicate ridges that are representative of major trends, and the symbol used to demark wrinkle ridges is also used to indicate simple ridges. Further, wrinkle ridges are not the only landforms on Mars that reflect crustal shortening. Features referred to as lobate scarps and high-relief ridges also appear to be contractional in origin.

Recent thermal history models for Mars suggest that the planet was initially hot and cooled monotonically over geologic time [*Schubert and Spohn*, 1990; *Schubert et al.*, 1993]. A long period of global contraction resulting from planetary cooling is predicted by such models and a global ridge system is often cited as evidence of global contraction [*Schubert and Spohn*, 1990; *Schubert et al.*, 1993; *Tanaka et al*, 1991; *Zimbelman et al.*, 1991]. The previous surveys do not provide a complete enough picture of compressional tectonism on Mars to evaluate these models.

In this study, contractional features on Mars are classified and mapped in a comprehensive survey of the planet. The spatial and temporal distribution of the contractional features is examined in an effort to understand the timing and extent of compressional tectonism. The patterns of the tectonic features and the geometry of the stresses inferred from the structures is analyzed and models for the origin of the stresses are discussed. The role of global contraction is also evaluated.

Paper number 93JE01138.

OBSERVATIONS

Wrinkle Ridges

Wrinkle ridges are structures with a complex morphology, often consisting of an assemblage of superimposed landforms (Figure 1). The morphologic elements consist of broad arches (up to 20 km wide) and narrow, asymmetric ridges (up to 6 km wide) [see *Watters*, 1988]. These sinuous and often regularly spaced landforms are generally attributed to folding and/or thrust faulting [*Bryan*, 1973; *Howard and Muehlberger*, 1973; *Muehlberger*, 1974; *Lucchitta*, 1976, 1977; *Maxwell et al.*, 1975; *Maxwell and Phillips*, 1978; *Sharpton and Head*, 1982, 1988]. Recent studies of terrestrial analogs support a compressional tectonic origin [*Plescia and Golombek*, 1986; *Watters*, 1988], although the relative role of folding and thrust faulting is still debated [*Golombek et al.*, 1991; *Watters*, 1991]. Strike-slip faulting may be associated with wrinkle ridges on Mars [*Schultz*, 1989] and with analogous structures on Earth and Venus [*Watters*, 1992]. Estimates of the average horizontal shortening across individual wrinkle ridges vary and are model dependent, but all are below 1 km [*Watters*, 1988; *Golombek et al.*, 1991].

Simple Ridges

Many landforms described as wrinkle ridges have been mapped in a variety of units other than ridged plains [*Chicarro et al.*, 1985; *Greeley and Guest*, 1987; *Scott and Tanaka*, 1986; *Tanaka and Scott*, 1987]. Examination of these features, using established criteria for describing wrinkle ridges [see *Watters*, 1988] reveals that, with few exceptions, they do not have the morphologic elements diagnostic of wrinkle ridges. They are interpreted to be a type of non-tectonic landform, referred to here as simple ridges.

Simple ridges are generally linear to sinuous, narrow, topographically positive features that may have a variety of origins. Many appear to be either erosional or depositional in nature. Examples of simple ridges resulting from erosion are found on Hellas Planitia (Figure 2a) were plains material has been deeply

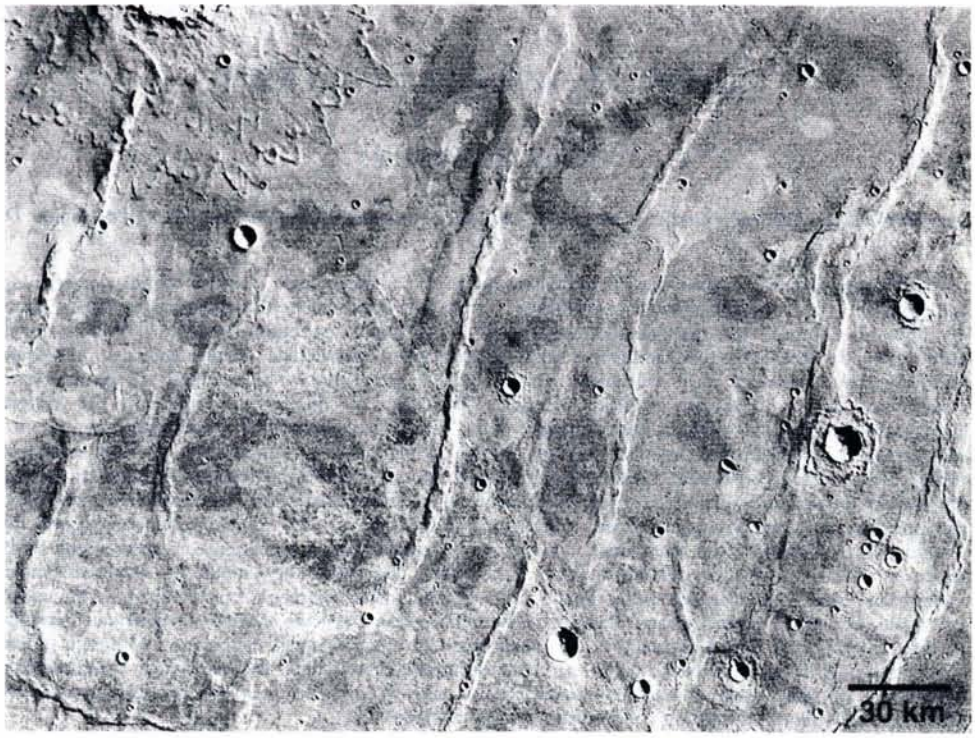

Fig. 1. Typical wrinkle ridges in ridged plains material of the Coprates region of the Tharsis province. Wrinkle ridges are comprised of an assemblage of landforms often superimposed on one another. The convergence of two wrinkle ridges into a semicircle (lower left) reflects the influence of a buried crater (Viking orbiter frames 608A24, 25, 26, 608A45).

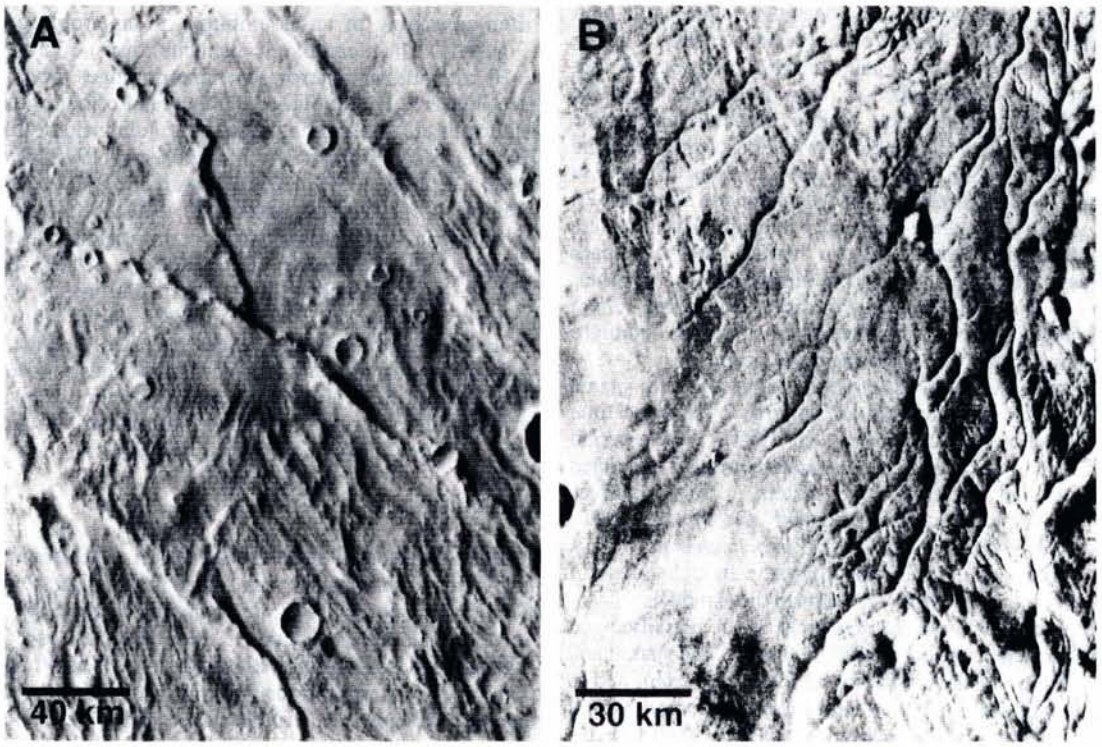

Fig. 2. Examples of simple ridges on Mars. Simple ridges in (a) Hellas Planitia (52°S, 301°W) and (b) Noachis Terra (Dorsa Argentea, 77°S, 35°W) are narrow, topographically positive features that may have resulted from either erosion or deposition (Viking orbiter frames 361S05 and 421B55).

dissected forming ridges and valleys oriented toward the center of the basin. These ridges may be the result of erosion by pyroclastic flows originating from Amphitrites Patera (R. Craddock, personal communication, 1991). In the south polar region, the Dorsa Argentea is comprised of a number of very narrow, highly sinuous simple ridges (Figure 2b). As pointed out by *Kargel and Strom* [1992], these features and others like them in the Argyre region and elsewhere on Mars have been interpreted to be inverted stream topography, spits or bars, exhumed igneous or clastic dikes or glacial eskers.

Lobate Scarps

Features described here as lobate scarps occur in cratered upland or highland material on Mars. These scarps are morphologically similar to highland scarps observed on the Moon and Mercury. In plan view, they are lobate, arcuate or linear and often segmented. In cross-section they are generally one-sided with either a level surface or one that is gently sloping away from the scarp. Many lobate scarps clearly deform crater floors and, like their counterparts on the Moon and Mercury, are interpreted to be the result of thrust faulting [*Lucchitta,* 1976; *Howard and Muehlberger,* 1973; *Binder,* 1982; *Binder and Gunga,* 1985; *Strom et al.,* 1975; *Cordell and Strom,* 1977]. A relatively large number of lobate scarps occur in the Noachian highland material of Terra Cimmeria, north of Hesperia Planum (Figure 3a). These scarps have roughly the same orientation as the steep structural and/or erosional scarp that marks the crustal dichotomy boundary in this area. Another area where lobate scarps are found is Noachis Terra. The scarps of this region, as well as others that occur in the highland material, are thought to be Noachian in age [*Greeley and Guest,* 1987; *Scott and Tanaka,* 1986]. However, this is difficult to determine with confidence because there are often no clear superposition relationships, and many of the scarps can be traced into and through crater floors. Lobate scarps in Memnonia (20°S, 160°W), on the southwestern flank of Tharsis, may have influenced the formation of some wrinkle ridges in smooth plains within impact craters [*Tanaka et al.,* 1991].

The average relief of the lobate scarps in Terra Cimmeria, north of Hesperia Planum, is estimated to be 300 m [*Watters et al.,* 1988]. The estimated horizontal shortening across an individual lobate scarp, assuming they are controlled by thrust faults dipping at roughly 30° [see *Byerlee,* 1978], is < 1 km. A few large-scale lobate scarps are also observed on Mars. One prominent example is Amenthes Rupes, located in Terra Cimmeria (2°N, 250°W) (Figure 3b). This scarp is approximately 400 km long and as much as 2.5 km high (based on shadow measurements). Another notable example is Eridania Scopulus located in southern Terra Cimmeria (55°S, 223°W). These scarps are comparable in scale to the Discovery Scarp on Mercury and may be the result of several kilometers or more of horizontal shortening.

High-Relief Ridges

High-relief ridges are estimated to be 1 to 3 km in height and occur in highland material. They are the most common in the highlands of Memnonia (20°S, 155°W), adjacent to units of ridged plains material [*Schultz,* 1985]. High-relief ridges are thought to be Noachian in age [*Scott and Tanaka,* 1986] and are much less abundant than the relatively low-relief wrinkle ridges (Figure 4a). They are interpreted to be tectonic in origin because they clearly deform crater floors [*Schultz,* 1985].

Although the origin of high-relief ridges is not well understood, linear or curvilinear features that appear to mark offsets in crater floors (see Figure 4a) suggest that either thrust or reverse faulting is involved. If high-relief ridges are controlled by thrust faults (dips ≤ 30°), there is no obvious explanation for the clear morphologic differences between these structures and lobate scarps, both of which occur in highland material. Another kinematic model that might account for the contrast in morphology and the greater relief of these ridges involves structural control by high-angle reverse faults. Estimates of the shortening across high-relief ridges is, as in the case of lobate scarps and wrinkle ridges, model dependent. Assuming they are controlled by thrust faults dipping at roughly 30°, the average horizontal shortening across individual structures in Memnonia is estimated to be roughly 4 km [*Forsythe et al.,* 1991]. If these features are controlled by high-angle reverse faults dipping at roughly 60°, the average horizontal shortening is on the order of 2.1 km.

Wrinkle Ridge-Scarp Transitions

The difference in style of deformation between the highland material and the ridged plains material is clearly demonstrated by structures referred to as wrinkle ridge-scarp transitions [*Watters et al.,* 1988, 1991]. These structures occur at the contact between smooth plains and highland material on the Moon and Mars. On the Moon they are found at the margins of mare basins and extend into adjacent highlands [*Lucchitta,* 1976]. In the smooth plains material the structures have a morphology typical of wrinkle ridges. Where the structures extend into the highlands, the morphology of the wrinkle ridge changes to that of a lobate scarp. A prominent wrinkle ridge-scarp transition occurs in Terra Cimmeria, in the area just northeast of Herschel basin. The smooth plains (presumably volcanic in origin) within a roughly 80 km diameter impact basin have been deformed into a wrinkle ridge (Figure 4b). Deformation can be traced along the trend of the ridge outside the basin into the adjacent uplands. In the highlands the morphology of the structure is clearly that of a scarp.

The contrast in the style of compressional deformation between smooth plains volcanic sequences and highland material may be explained by a contrast in the mechanical properties of the materials [*Watters et al.,* 1988], specifically the presence or absence of layering [*Watters et al.,* 1991]. A multilayer will tend to fold when contacts are frictionless or have low yield strengths, or fault when contacts are welded and the material behaves like a single layer [*Johnson,* 1980]. This is consistent with the suggestion that differences in the strength of the materials may contribute to the contrast in morphology between wrinkle ridges and scarps [*Tanaka et al.,* 1991].

Long Wavelength Folds

Other significant forms of compressional deformation that are not expressed by distinct morphologic features that can be characterized by photogeologic studies may be present on Mars. One such feature may result from buckling of the lithosphere [*Watters,* 1987; 1991; *Zuber and Aist,* 1990]. Possible examples of long wavelength, low amplitude folds are revealed in Earth-based radar altimetry profiles across the Tharsis rise (south of Valles Marineris). They appear as broad topographic undulations with a maximum relief of 1 km [*Watters,* 1987; *Schultz and Tanaka,* 1992]. In contrast to the relatively short length-scale exhibited by regularly spaced wrinkle ridges (average 30 km), these features have spacings on the order of 400 km. Such long wavelength structures should be clearly resolved by the Mars Observer Laser Altimeter [see *Zuber et al.,* 1992].

Survey of Contractional Features

Applying the criteria described above for classifying a landform either as a wrinkle ridge, lobate scarp or a high-relief ridge, a survey of these tectonic features was made using the 1:2 million-scale controlled photomosaics and individual Viking Orbiter images. Data sets were compiled by digitizing the outline of the structures directly from the photomosaics. The structures were divided into segments with roughly uniform orientations generally greater than 5 km in length. Over 3,900 segments were

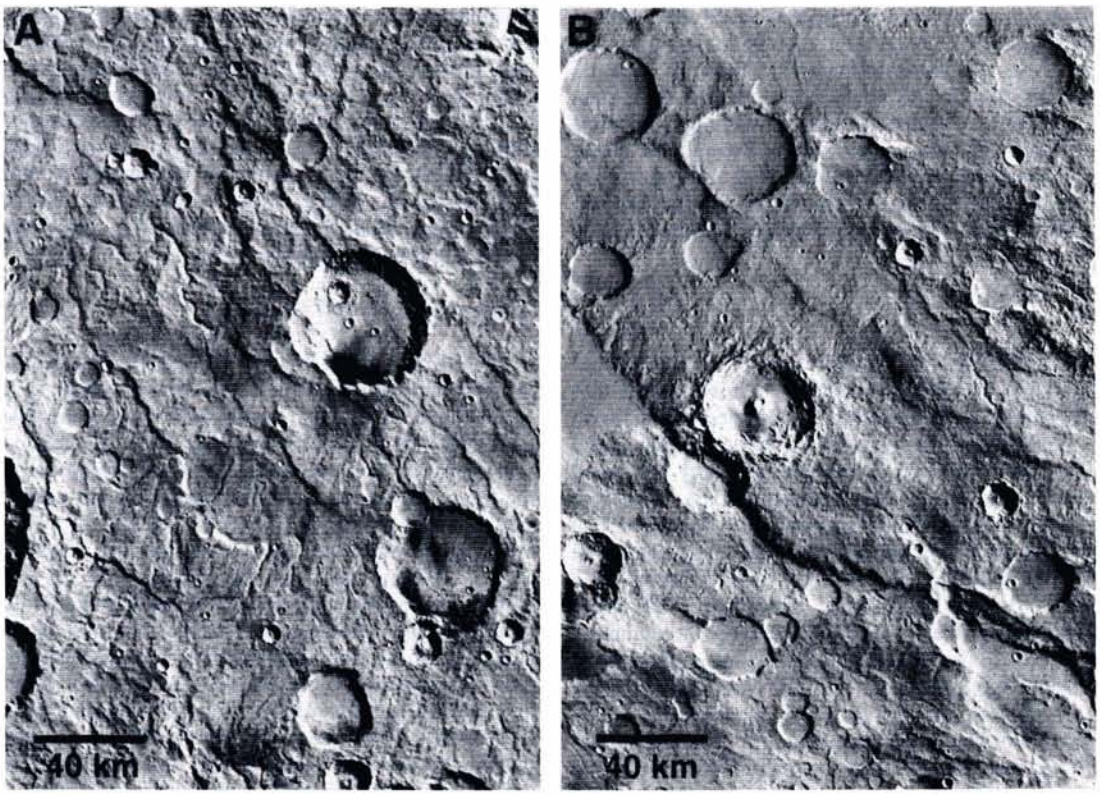

Fig. 3. Lobate scarps on Mars. (a) Lobate scarps in Terra Cimmeria (6°S, 235°W) occur in highland material and appear to be the result of thrust faulting (Viking orbiter frames 637A52, 54; 629A21, 22, 23, 24, 381S81, 82). (b) Amenthes Rupes, also located in Terra Cimmeria (2°N, 250°W), is a large-scale lobate scarp that resulted from several kilometers or more of horizontal shortening (Viking orbiter frames 878A15, 878A17, 878A48, 381S41, 381S42, 379S46).

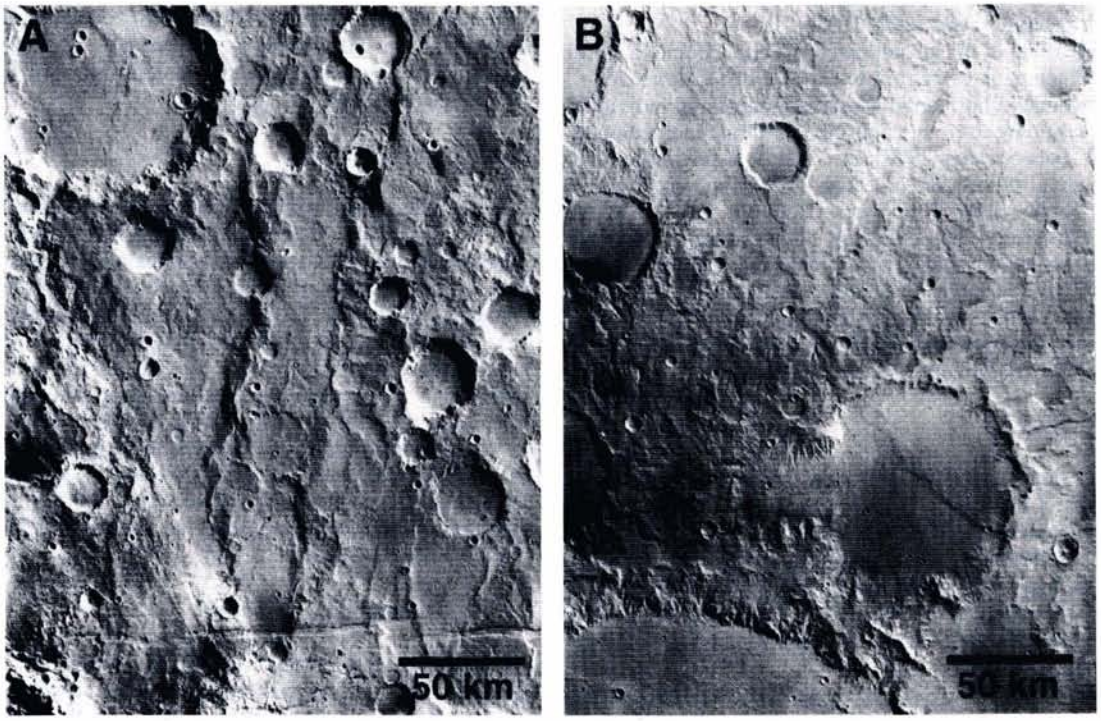

Fig. 4. High-relief ridges and wrinkle ridge-lobate scarp transitions. (a) High-relief ridges in Memnonia (12°S, 165°W) occur in highland material and may be the result of reverse or thrust faulting (Viking orbiter frames 599A61, 76, 78). (b) The wrinkle ridge in the smooth, presumably volcanic plains in a impact basin north of Herschel basin (lower left) and the lobate scarp in the adjacent highlands are parts of a continuous structure that reflects the contrast in style of compressional deformation between the two materials (Viking orbiter frames 629A26, 43, 381S81, 83).

digitized and coded according to the type of structure and the geologic unit in which it occurs.

It is clear from this survey that contractional features on Mars are not uniformly distributed spatially (Plates 1 and 2) or temporally. Compressional deformation is most prevalent in ridged plains material that are Early Hesperian (Hr) and Middle to Late Noachian (Nplr) in age [see *Scott and Tanaka,* 1986; *Greeley and Guest,* 1987; *Tanaka and Scott,* 1987]. Wrinkle ridges are the predominant contractional feature in ridged plains. The largest concentration of wrinkle ridges occurs in the ridged plains units of Hesperia Planum (eastern hemisphere) and in Coprates and Lunae Planum (western hemisphere)(Plates 1and 2). Lobate scarps are the dominant contractional feature in highland material (i.e., Npl_1, Npl_2, Npld). Wrinkle ridges are not observed in highland material. Examining the cumulative length of the mapped contractional features, wrinkle ridges account for about 81% of the total, followed by lobate scarps at about 18% and high-relief ridges at about 1% (Table 1). This survey also indicates that the vast majority of the contractional features on Mars (i.e., lobate scarps and wrinkle ridges) are the results of a relatively small amount of distributed horizontal shortening.

Patterns of Tectonic Features and Inferred Stresses

The patterns of the contractional features and the stresses inferred from these structures were analyzed in the eastern and western hemisphere. The geometry of the inferred stresses were examined by fitting great circles, representing traces along the surface of a principal stress trajectory, to each segment and plotting them on a Schmidt net [*Guth,* 1987]. The direction of the principal stresses are inferred from the orientation of the structure (σ_1 is assumed to be horizontal and normal to the trace of the structure) [see *Golombek,* 1989; *Watters et al.,* 1990]. A perfect radially symmetric system results in a concentration of intersections near 100% per 1% area of the net. Randomly generated points will yield randomly distributed concentrations that decrease in significance with increasing sample size [see *Stauffer,* 1966]. Although this method is useful in identifying systems with radial symmetry, concentrations do not uniquely reflect the existence of such systems.

The most distinctive pattern of contractional features in the western hemisphere is formed by the well known circum-Tharsis wrinkle ridge system (Plate 1) [see *Wise et al.,* 1979; *Watters and Maxwell,* 1986]. Intersections of great circles fit to all segments of the contractional features in the western hemisphere (n = 2253) are distributed in a broad, discontinuous band, trending roughly northeast-southwest (Figure 5a) with a maximum concentration of 5.1% per 1% area centered between Pavonis Mons and Syria Planum (~6°S, 108°W). The location and significance of this center does not change appreciably even if only the longest segments (≥30 km, n = 450) are analyzed (maximum concentration 6.7% at ~0°N, 117°W). This is generally consistent with the results of other studies of the geometry of the inferred stresses using data sets comprised of only wrinkle ridges associated with the Tharsis province [*Wise et al.,* 1979; *Watters and Maxwell,* 1986; *Golombek,* 1989; *Watters et al.,* 1990].

Many of the contractional features in the western hemisphere, however, are not circumferential to a point in central Tharsis. The secondary concentration of intersection located in northern Lunae Planum (~16°N, 61°W) is due largely to northwest-southeast to east-west trending wrinkle ridges in Coprates (25°S, 69°W) and southern Lunae Planum (1°S, 72°W) that transect ridges with circumferential orientations. In other areas such as Memnonia, many of the scarps and high-relief ridges [see *Schultz,* 1985], as well as some wrinkle ridges, do not have orientations circumferential to central Tharsis. The most notable deviations from the Tharsis circumferential trend are found in the ridged plains and highlands northeast of Argyre Planitia in Noachis Terra (40°S, 15°W) (Plate 1). Contractional features in this region have a dominant northwest trend, somewhat radial to Tharsis and concentric to Argyre [see *Chicarro et al.,* 1985].

In contrast to the western hemisphere, contractional features in the eastern hemisphere demonstrate strong local and regional-scale trends but no patterns that are significant on the hemispheric-scale. Intersections of great circles fit to all the contractional features in the eastern hemisphere (n = 1674) are distributed in a continuous, somewhat sigmoidal northwest-southeast trending band (Figure 5b) with a maximum density of 11.2% located in Hesperia Planum (~25°S, 245°W). The relatively strong concentration in Hesperia Planum is primarily the result of the dense population and localized nature of the wrinkle ridges in this area (Plate 2). Many form a roughly circular or arcuate pattern that is transected by northeast and northwest trending ridges and, to a lesser extent, by north-south and east-west trending ridges. The cross-striking wrinkle ridges in Hesperia and elsewhere on Mars form what has been termed a reticulate ridge pattern (Figure 6) [see *Raitala,* 1988; *Watters and Chadwick,* 1989].

Wrinkle ridges and lobate scarps in ridged plains and highlands material of Terra Cimmeria (40°S, 200°W) exhibit a parabola-like regional trend (Plate 2). In southern Terra Cimmeria, these features have a dominant northeast trend, whereas further north, this trend becomes north-northwest to northwest, parallel to the trend of the scarp that marks the crustal dichotomy. This northwest trend is shared by contractional features in ridged plains and highland material of Syrtis Major (10°N, 290°W) and Arabia Terra (30°N, 330°W)(Plate 2). Northeast trending wrinkle ridges are observed in ridged plains of Elysium Planitia (10°N, 230°W) as well as Hesperia Planum. As noted by *Scott and Dohm* [1990], this northeast trend parallels the alignment of Hadriaca Patera, Tyrrhena Patera, Elysium Mons, and Hecates Tholus, although the importance of this alignment is not clear.

DISCUSSION

Implications for the Thermal and Tectonic History

From estimates of the total area resurfaced by volcanic material as a function of age [*Tanaka et al.,* 1988; *Greeley and Schneid,* 1991], there seems to be little doubt that the Early Hesperian was a period that experienced a major pulse of volcanism (Figure 7). Estimates range from 37% [*Tanaka et al.,* 1988] to 41% [*Greeley and Schneid,* 1991] to over 50% [*Frey,* 1992] of the planet resurfaced in a period lasting either approximately 100 million (3.8 to 3.7 b.y. ago [*Neukum and Wise,* 1976]) or 400 million years (3.5 to 3.1 b.y. ago [*Hartmann et al.,* 1981; *Tanaka,* 1986]). In fact, the Early Hesperian appears to have been the most significant period of volcanism in the geologic history of Mars after the Early Noachian [*Greeley and Schneid,* 1991; *Frey,* 1992].

Thermal history models that are based on an initially hot, entirely differentiated planet predict an early period of rapid cooling of the interior lasting several hundred million to a billion years, followed by slow cooling throughout the rest of the geologic history [*Schubert and Spohn,* 1990; *Schubert et al.,* 1993]. These models also predict that the average rate of volcanism will decrease monotonically with time. Such a decline is inconsistent with estimates of total area (Figure 7) and average rate of volcanic resurfacing during the Early Hesperian [see *Zimbelman et al.,* 1991; *Frey,* 1992]. In contrast to the models of *Schubert and Spohn* [1990] and *Schubert et al.* [1993], *Stevenson and Bittker* [1990] argue that heat loss due to volcanism could have a stabilizing effect on mantle convection resulting in long periods of reduced volcanic activity. This, in turn, results in heating of the interior that would lead to an episode of widespread volcanism. Future models of the thermal history of Mars must accommodate the observed peak in volcanic activity during the Early Hesperian.

The thermal history is, of course, coupled to the tectonic history. During the period of rapid planetary cooling predicted in the models of *Schubert and Spohn* [1990] and *Schubert et al.*

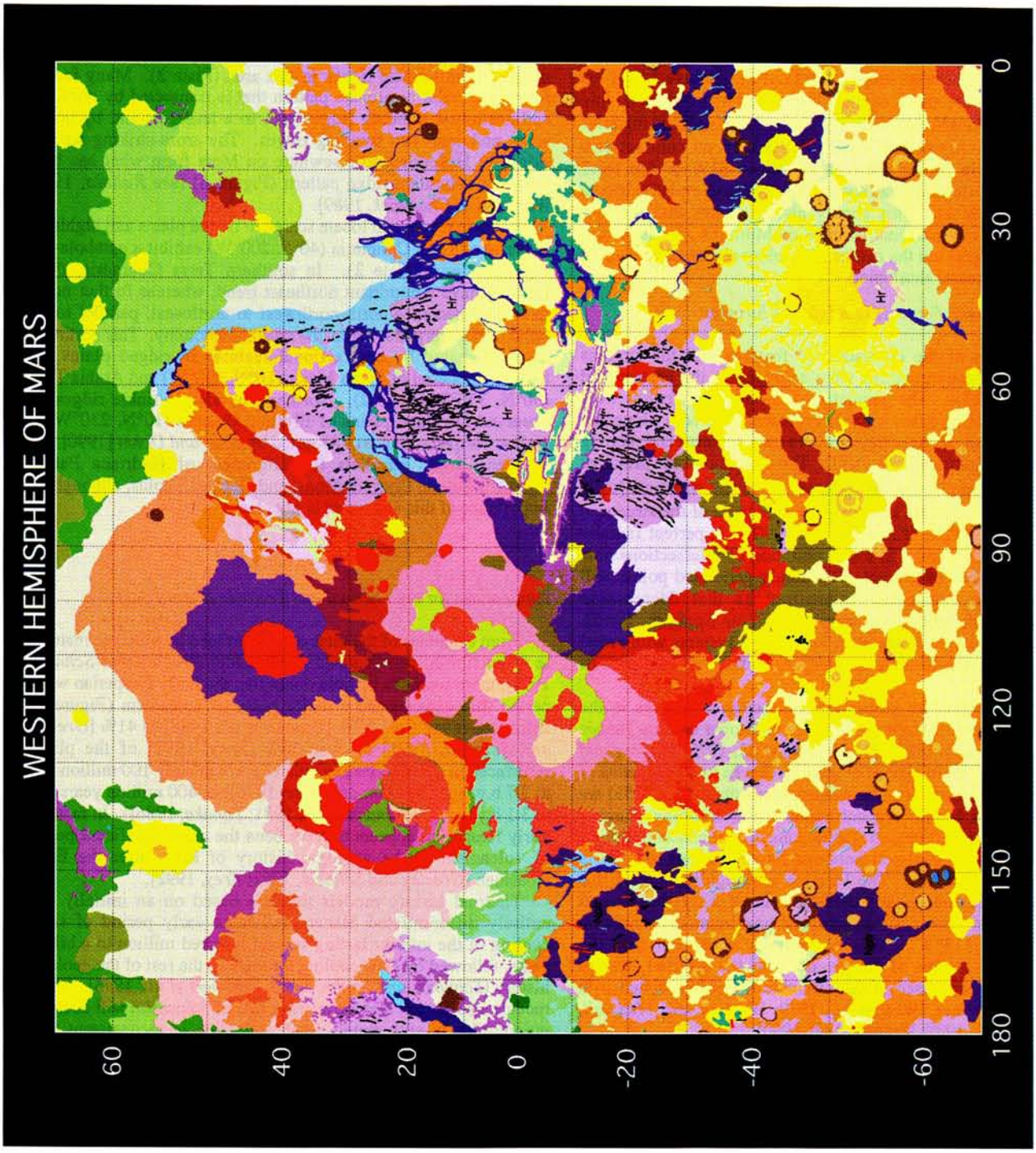

Plate 1. Contractional features in the western hemisphere. Digitized segments of wrinkle ridges (black lines), lobate scarps (cyan-blue lines) and high-relief ridges (red lines) are overlaid on the geologic map of Mars compiled by *Tanaka et al.* [1988]. Unit colors approximate those used in the 1:15,000,000 geologic map series of the western hemisphere and the poles [*Scott and Tanaka*, 1986; *Tanaka and Scott*, 1987].

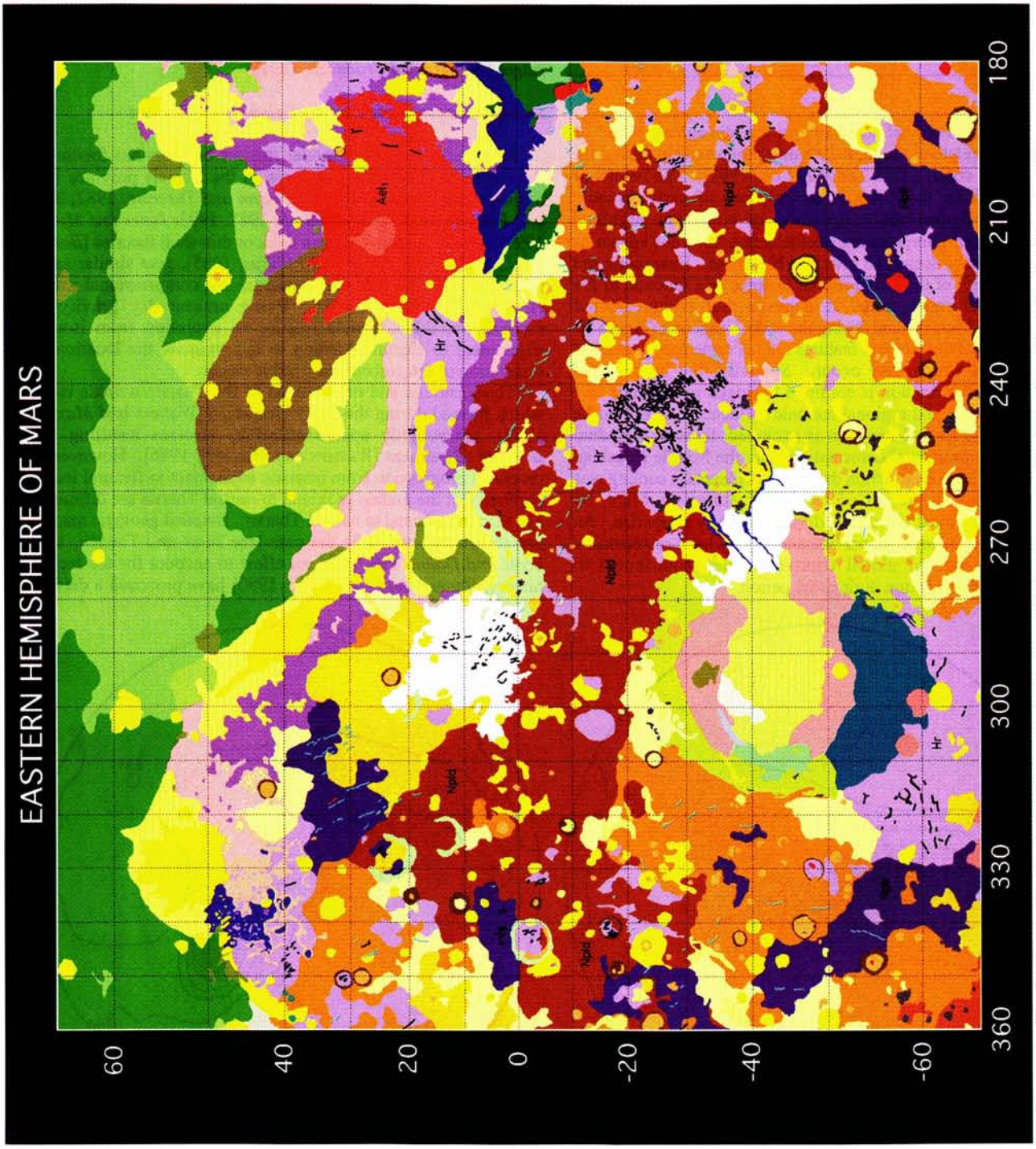

Plate 2. Contractional features in the eastern hemisphere. Digitized segments of wrinkle ridges (black lines), lobate scarps (cyan-blue lines) and high-relief ridges (red lines) are overlaid on the digital geologic map of Mars compiled by *Tanaka et al.* [1988]. Unit colors approximate those used in the 1:15,000,000 geologic map series of the eastern hemisphere and the poles [*Greeley and Guest*, 1987; *Tanaka and Scott*, 1987].

TABLE 1. Cumulative Lengths of Contractional Features on Mars

Tectonic Feature	Total Length (km)	Segments
Wrinkle Ridges	71,926	3,130
Lobate Scarps	16,105	744
High-Relief Ridges	1,096	53

[1993], the compressional strain rate in the lithosphere would be expected to be relatively high, decreasing progressively during the period of slow cooling [see *Tanaka et al.*, 1991]. The results of this study indicate that there is no evidence of early, broadly distributed compressional tectonism in Noachian highland material. Further, compressional deformation does not appear to have progressively decreased after the Noachian. Examining the cumulative length of the contractional features as a function of the age of the deformed units, it appears that compressional deformation on Mars peaked during the early Hesperian (Figure 8). This assumes that the tectonic features are the same age, generally, as the units in which they occur. Spatially, the bulk of the compressional deformation is confined to ridged plains units that reflect strong local and regional tectonic influences. It should be noted that if the Early Hesperian is excluded, there is a gradual decrease in compressional deformation from the Middle Noachian (Figure 8). If global contraction due to rapid planetary cooling was important in the formation of tectonic features on Mars, its influence was the most significant during the Early Hesperian. An Early Hesperian pulse of global volcanism may have resulted in a punctuated episode of global contraction that contributed to compressional deformation during that period.

The only significant compressional deformation after the Early Hesperian occurs on a local-scale in Upper Hesperian flows of Syrtis Major Planum (Hs) and in dispersed Upper Hesperian smooth plains volcanic material (Hpl_3)(see Plates 1 and 2). Relatively few contractional features are found in volcanic plains dated as Amazonian in age. Some wrinkle ridges are found in Lower Amazonian volcanic flows attributed to Elysium Mons (Ael_1)(Plate 2; 20°N, 200°W). A small number of Amazonian age wrinkle ridges are found in the floor material of Kasei Valles. These are distinguishable from other generally heavily degraded ridges that are probably erosional remnants of preexisting wrinkle ridges [*Watters and Craddock*, 1991].

Implications for Models for the Origin of the Stresses

Much of the effort to model stresses on Mars has focused on the origin of the tectonic systems in the Tharsis province [e.g., *Solomon and Head*, 1982; *Willemann and Turcotte*, 1982; *Sleep and Phillips*, 1985; *Banerdt et al.*, 1982, 1993; *Janes and Melosh*, 1990]. Those models based on thick or thin shell theories [*Banerdt et al.*, 1982, 1993; *Sleep and Phillips*, 1985], give similar results with respect to the predicted tensional and compressional stresses [see *Banerdt et al.*, 1993]. Using present day gravity and topography, these models require an evolution from isostatic adjustment to flexural loading to approximate the location and orientation of the graben and wrinkle ridges.

The locations and orientations of the Tharsis wrinkle ridges, which formed during the Early Hesperian [*Watters and Maxwell*, 1983], are roughly approximated by stresses resulting from isostatic adjustment [*Watters and Maxwell*, 1986]. However, the proposed progression from isostatic adjustment to flexural loading requires that the graben proximal to central Tharsis are different in age than those distal to central Tharsis. Detailed geologic mapping has shown this not to be the case [see *Scott and Tanaka*, 1986; *Scott and Dohm*, 1990]. In an effort to account for the tectonic history, *Banerdt and Golombek* [1990] have proposed a detached

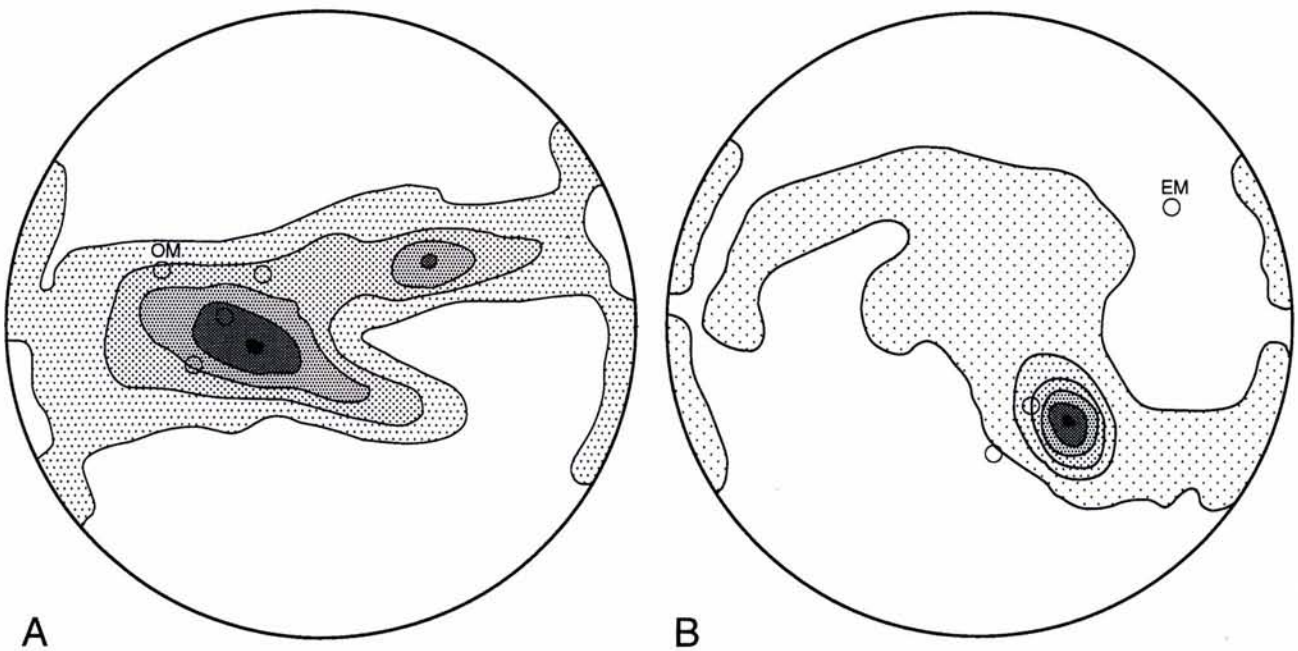

Fig. 5. Beta diagrams showing the concentration of intersecticns of great circles fit to the inferred maximum principal stress direction (σ_1) of segments of contractional features. The number of intersections (N) is equal to n(n-1)/2 where n is the number of great circles plotted. (a) In the western hemisphere, contours indicate 1, 2, 3, 4 and 5% per 1% area (N = 2,536,878) with a maximum density of 5.1% located in an area between Pavonis Mons and Syria Planum at approximately 6°S, 108°W and a secondary concentration located in the area of central Lunae Planum at approximately 16°N, 61°W. Olympus Mons (OM) and the Tharsis Montes volcanoes (circles) are shown as reference points. (b) In the eastern hemisphere contours indicate 1, 3, 5, 7, 9 and 11% per 1% area (N = 1,400,301) with a maximum concentration of 11.2% located in Hesperia Planum at approximately 25°S, 245°W. Elysium Mons (EM) and Tyrrhena and Hadriaca Patera (circles) are shown as reference points.

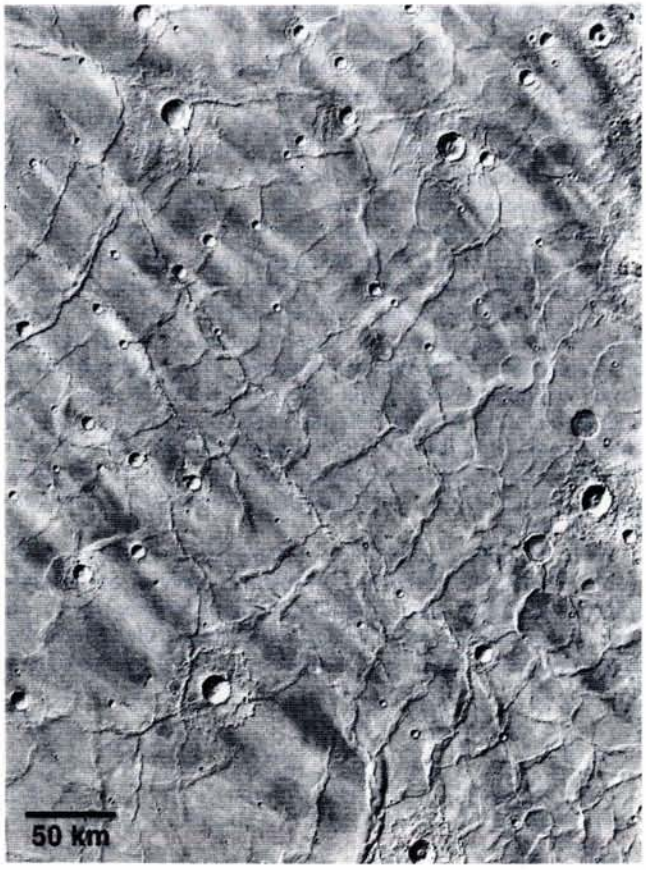

Fig. 6. Wrinkle ridges in the plains of Hesperia Planum. Cross-striking northeast and northwest trending ridges form an intricate, reticulate pattern. Numerous circular wrinkle ridges clearly indicate the influence of buried craters on the formation of these structures and the importance of subsidence (Viking orbiter frames 356S64-68).

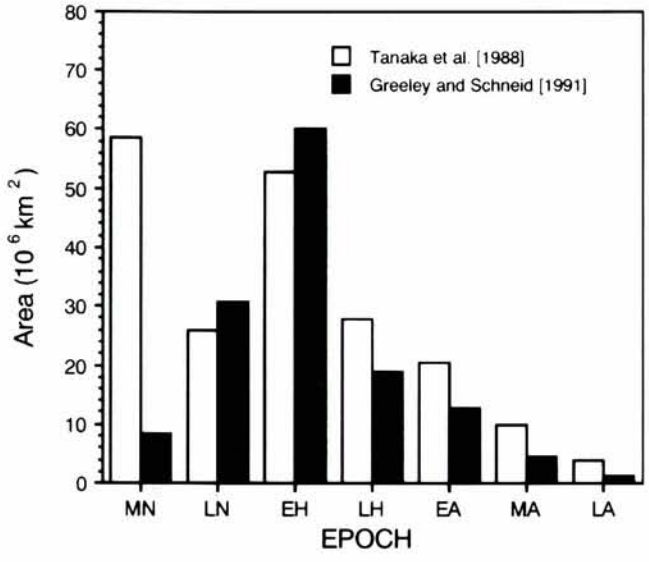

Fig. 7. Histogram of the total area resurfaced by volcanic material as a function of age. Estimates of *Tanaka et al.* [1988] and *Greeley and Schneid* [1991] consist of the total area covered by volcanic material, both exposed and buried.

crustal cap model [also see *Tanaka et al.*, 1991]. In this model the brittle upper crust in the central Tharsis region is decoupled from the rest of the lithosphere as a result of higher heat flow and a thicker crust in this area [see *Solomon and Head*, 1990]. Under these conditions, the lithosphere in the Tharsis region deforms as part of the globally continuous shell, and the thin crustal layer deforms as a spherical cap with a lubricated lower surface. The peripheral boundary of the cap is welded or fixed to the global shell. *Banerdt and Golombek* [1990] argue that radial extension within the cap will result from isostatic spreading forces and increases in the radius of curvature induced by subsidence of the lower lithosphere. Beyond the boundary of the decoupled crust, distal radial extension is consistent with earlier flexural loading models. Some radial compression is predicted for the periphery of the Tharsis rise [*Tanaka et al.*, 1991], perhaps concentrated near the transition zone [Banerdt and *Golombek*, 1990]. *Tanaka et al.* [1991] attribute the circumferential wrinkle ridge system on the edge of the Tharsis rise to global compressional stresses augmented by increased peripheral compression from isostatic relaxation stresses.

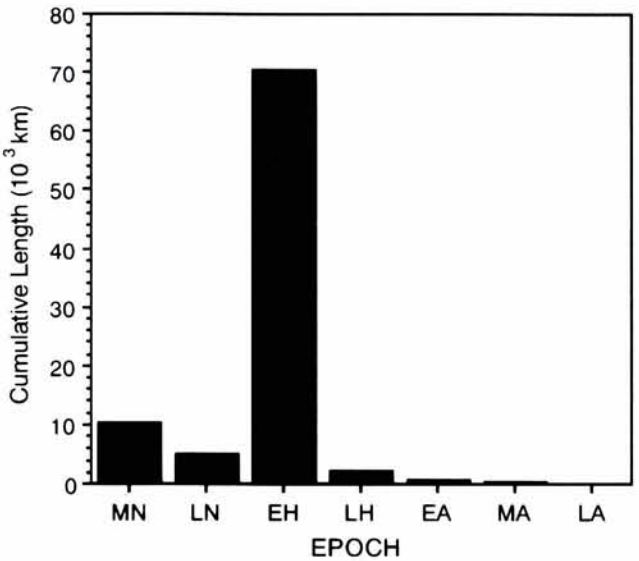

Fig. 8. Histogram of the cumulative length of contractional features as a function of the age of the deformed units. Mapped segments of wrinkle ridges, lobate scarps and high-relief ridges were coded according to the units in which they occur and the lengths of the three features were totaled for each Martian epoch.

In contrast to the predictions of this model, however, wrinkle ridge formation was probably not confined to the edge of the Tharsis rise [*Watters and Maxwell*, 1986]. Only the apparent extent of compressional deformation can be determined from the location of the wrinkle ridges. Although the true extent of the ridge system is obscured by post ridged plains volcanism and erosion, the nature of the contacts between the units suggests that ridged plains and wrinkle ridges extended further onto the Tharsis rise than is presently observed. Thus, models for the origin of the stresses in the Tharsis province must account for the following: (1) wrinkle ridges formed during the Early Hesperian, prior to the development of the radial faults that cut the ridged plains; (2) the wrinkle ridge system likely extended further onto the Tharsis rise than is presently observed; (3) wrinkle ridges and other contractional features in the western hemisphere are only roughly circumferential in nature (inferred stress directions weakly radial to a Pavonis Mons-Syria Planum center); and (4) the rotation of stresses resulting in cross-striking ridges forming reticulate patterns in some areas.

Horizontally isotropic stresses due to global contraction of the Martian interior may have been a significant component of the total stresses [see *Sleep and Phillips*, 1985], particularly in the eastern hemisphere. Introducing stresses due to global contraction has

important implications for the origin of the tectonic features. In the case of uniform cooling of an initially hot sphere with homogenous, isotropic properties, no deviatoric stress is generated. The state of stress that results is one of hydrostatic compression (all three principal stresses equal in magnitude and sign). A cooling planet is different. The lithosphere is already cold and cannot cool much more, thus the bulk of the heat loss is from the interior. The cool lithosphere, which alone is capable of supporting deviatoric stresses, adjusts to the decreasing volume of the interior under the influence of gravity. The horizontal stresses increase in magnitude while the vertical stress remains ρgz. This excludes the influence of thermal elastic stresses resulting from heating of the lithosphere. If the contractional features (i.e., wrinkle ridges, lobate scarps and high-relief ridges) are the result of reverse or thrust faulting, global contraction would contribute to the stress difference between the vertical and horizontal components necessary to initiate shear failure (Figure 9). If wrinkle ridges are folds with thrust faults developed as a consequence of folding, global contraction may provide the critical horizontal stress necessary to initiate buckling.

Although the stresses resulting from global contraction may have been necessary to generate many of the tectonic features, they are not sufficient. Because global contraction results in horizontal stresses that are equal in magnitude, contractional features would be expected to occur in random or disorganized [see *Janes and Melosh*, 1990] patterns rather than with the uniform orientations observed on the local and regional scale. This is unless inhomogeneities in the stress field allow a sufficient difference between the horizontal components for one to be maximum and the inhomogeneity is uniform on those scales, a condition that is not likely to exist. In order to generate the uniform orientations, stresses resulting from global contraction must be superposed on nonhydrostatic horizontal stresses. Thus nonhydrostatic horizontal stresses, derived from local and/or regional sources, are required.

An important source of local and regional compression may be subsidence. Subsidence may have played a particularly significant role in the eastern hemisphere, beyond the influence of the Tharsis, where wrinkle ridges occur in ridged plains material that occupies topographic lows in the Martian highlands. Compressional stresses due to subsidence may result from either crustal cooling and volume reduction, loading from the ridged plains material or both [see *Raitala*, 1987, 1988; *Wilhelms and Baldwin*, 1989; *Watters and Chadwick*, 1989]. Subsidence may have been facilitated by magma-ice interactions within the highland material [*Wilhelms and Baldwin*, 1989].

As in the case of subsidence of Mare basalts in basins on the Moon, discontinuities in the subsurface, such as basin rings, influence and often localize the formation of wrinkle ridges. On Mars, this is demonstrated by ridges that reflect the influence of buried craters. These circular ridges, localized by the rims of

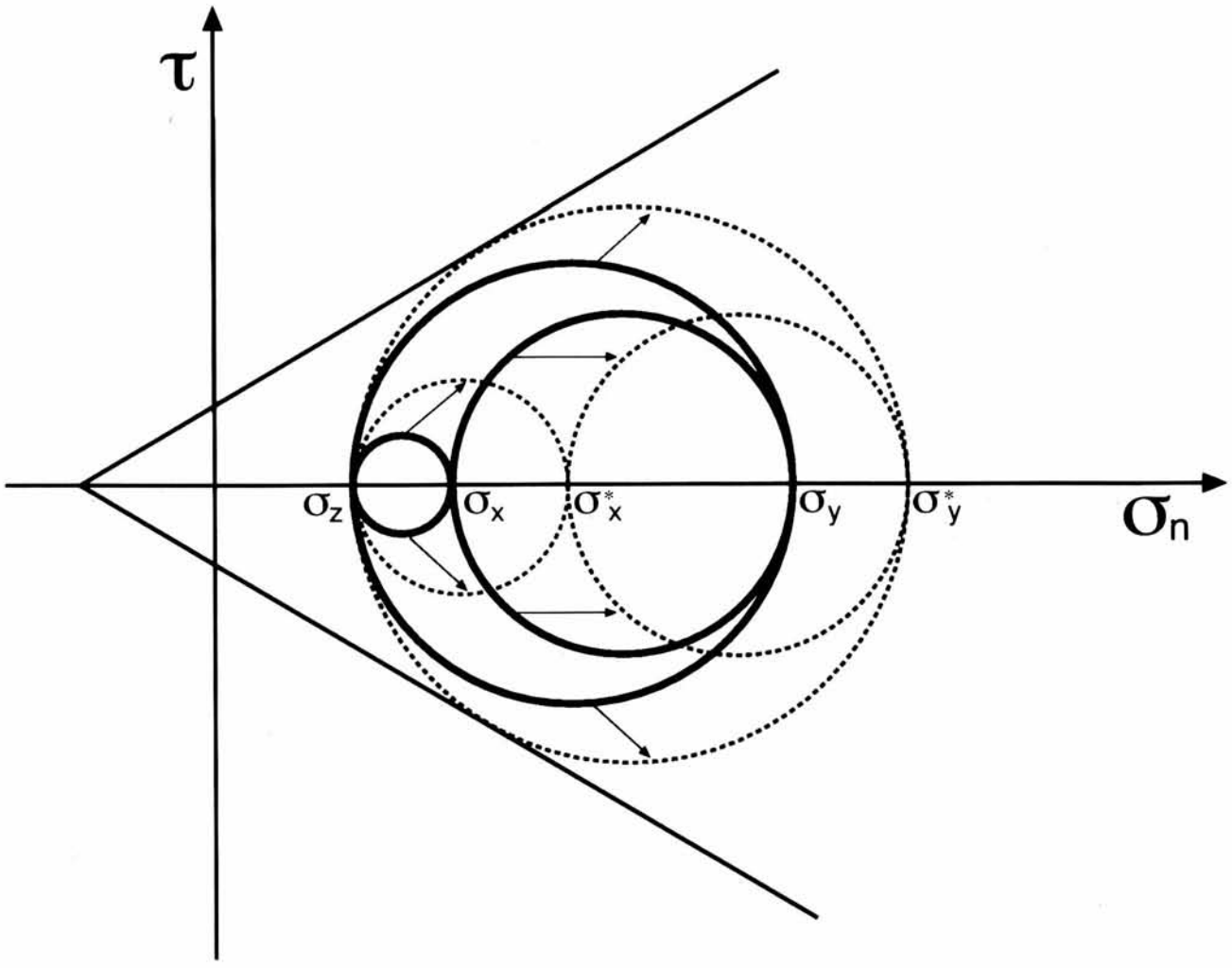

Fig. 9. Mohr diagram illustrating the effect of stresses resulting from global contraction superposed on a state of nonhydrostatic compression. Global contraction results in an increase in the horizontal stresses (σ_x, σ_y) while $\sigma_z = \rho gz$ remains constant. Note that $\sigma_y - \sigma_x$ and $\sigma^*_y - \sigma^*_x$ also stay constant. The stress difference ($\sigma^*_y - \sigma_z$) necessary to initiate thrust faulting can be achieved through global contraction.

craters formed in the substrate, are common in ridged plains units in both the eastern and western hemispheres. They are particularly prominent in the ridged plains of Hesperia Planum (Figure 6). Models that assume wrinkle ridges on Mars result from thick-skinned deformation involving thrust faults that penetrate most of the lithosphere [*Golombek et al.*, 1990; *Zuber and Aist*, 1990; *Tanaka et al.*, 1991] must account for the obvious sensitivity of wrinkle ridges to local, shallow-depth mechanical inhomogeneities introduced by underlying buried craters.

Another mechanism that has been suggested for generating compressional stress on Mars is the removal of overburden through erosion. If the material behaves elastically and is laterally confined, horizontal compression will result from the removal of a substantially thick section of material [*Turcotte and Schubert*, 1982; *Watters and Craddock*, 1991]. *Tanaka et al.* [1991] suggest that compressional features in the highlands resulted from global contraction augmented by compression due to erosion of highland materials during the Late Noachian and Early Hesperian. This is possible only if the material eroded from the highlands has been largely removed rather than redistributed locally [see *Craddock and Maxwell*, 1990, 1993]. However, the relatively uniform orientations of the contractional features can not be explained by stresses due to loss of overburden and global contraction alone. This is because loss of overburden results in horizontal principal stresses that are equal in magnitude [see *Turcotte and Schubert*, 1982], assuming that the mechanical properties of the material are homogeneous and isotropic. Again, the pattern of the structures would be expected to be disorganized. As in the case of global contraction, an additional nonhydrostatic source of stress is necessary. In the Kasei Valles, where as much as 2 km or more of material has clearly been removed, compressional stresses resulting from loss of overburden are significant [*Tanaka et al.*, 1991; *Watters and Craddock*, 1991]. These stresses coupled with residual compressional stresses related to Tharsis may explain the location and orientation of wrinkle ridges in the floor material of Kasei Valles.

SUMMARY

In a survey of contractional features on Mars, three morphologically distinct classes of structures have been mapped, wrinkle ridges, lobate scarps and high-relief ridges. These landforms are interpreted to be tectonic in origin based on photogeologic evidence of crustal shortening and comparisons with terrestrial and planetary analogs. Landforms referred to as simple ridges have been grouped with contractional features in previous surveys. Simple ridges, however, lack the morphologic elements that characterize contractional features and appear to be the result of erosion or deposition.

Contractional features on Mars are not uniformly distributed spatially or temporally. Wrinkle ridges account for over 80% of the total cumulative length of the mapped features and occur almost exclusively in smooth plains volcanic material. Lobate scarps account for 18% of the contractional features, occurring almost exclusively in highland material. The contrast in the style of deformation between smooth plains and highland material is reflected by wrinkle ridge-lobate scarp transitions, rare structures that occur at the contact between the two materials.

The pattern of contractional features in the western hemisphere clearly reflects the influence of the Tharsis rise, although this influence is not homogeneous. The eastern hemisphere has no dominant hemispheric-scale tectonic pattern, however, regional-scale patterns are observed. Contractional features with orientations that parallel the trend of the crustal dichotomy in the eastern hemisphere suggest the influence of regional stresses related to its development.

Assuming tectonic features are roughly the same age as the units in which they occur, compressional deformation peaked during the Early Hesperian. This corresponds to an Early Hesperian peak in the area resurfaced by volcanic material. Thermal history models for Mars, based on an initially hot planet, predict an early, long-lived period of rapid cooling and planetary contraction. In these models, the remainder of the geologic history of the planet is characterized by slow cooling of the interior and a monotonic decrease in volcanism and the lithospheric strain rate. Estimates of the timing of peak compressional tectonism and of the rate of volcanism are inconsistent with these models. An Early Hesperian pulse of global volcanism may have resulted in a punctuated episode of rapid cooling and global contraction that contributed to compressional tectonism during that period.

The compressional deformation of crustal materials on Mars may have involved stresses from local, regional and global-scale sources. Regional-scale tectonic stresses and local-scale stresses resulting from subsidence, and possibly other sources, may have been augmented by global contraction. Horizontally isotropic stresses due global contraction may have contributed an important component of the total stresses, however, they are not sufficient to account for the uniform orientations of the tectonic features.

Acknowledgments. I thank Richard A. Schultz, a anonymous reviewer and Daniel M. Janes for their valuable insights and guidance. I also thank Norman H. Sleep for his guidance in assessing the influence of global contraction and in the preparation of Figure 9. I also thank Michael J. Tuttle and Robert A. Craddock for their assistance in data collection and Michael J. Tuttle and Jeffrey K. Wade for preparing the plates and figures. This research was supported by NASA Planetary Geology and Geophysics Program grants NAGW-940 and NAGW-1106.

REFERENCES

Banerdt, W.B., R.J. Phillips, N.H. Sleep, and R.S. Saunders, Thick shell tectonics on one-plate planets: Applications to Mars, *J. Geophys. Res., 87*, 9723-9733, 1982.

Banerdt, W.B., M.P. Golombek, and K.L. Tanaka, Stress and tectonics on Mars, in *Mars*, edited by H.Kieffer, B. Jakosky, C. Snyder, and M. Matthews, pp. 249-297, University of Arizona Press, Tucson, 1993.

Banerdt, W.B., and M.P. Golombek, The evolution of Tharsis: Implications of gravity, topography, and stress (abstract), *Lunar Planet. Sci. Conf., XXI*, 54-55, 1990.

Binder, A.B., Post-Imbrian global lunar tectonism: Evidence for an initially totally molten moon, *Earth Moon Planets, 26*, 117-133, 1982.

Binder, A.B., and H.-C. Gunga, Young thrust-fault scarps in the highlands: Evidence for an initially totally molten moon, *Icarus, 63*, 421-441, 1985.

Bryan, W.B., Wrinkle-ridges as deformed surface crust on ponded mare lava, *Geochim. Cosmochim. Acta, 1, suppl., 93*, 106, 1973.

Byerlee, J.D., Friction of rocks, *Pure Appl. Geophys., 116*, 615-626, 1978.

Chicarro, A.F., P.H. Schultz and P. Masson, Global and regional ridge patterns on Mars, *Icarus, 63*, 153-174, 1985.

Cordell, B.M., and R.G. Strom, Global tectonics of Mercury and the Moon, *Phys. Earth Planet. Inter., 15*, 146-155, 1977.

Craddock, R.A., and T.A. Maxwell, Resurfacing of the Martian Highlands in the Amenthes and Tyrrhena region, *J. Geophys. Res., 95*, 14,265-14,278, 1990.

Craddock, R.A., and T.A. Maxwell, Geomorphic evolution of the Martian highlands through ancient fluvial processes, *J. Geophys. Res., 98*, 3453-3468, 1993.

Forsythe, R.D., R.A. Schultz and T.R. Watters, Distributed low strain regimes of the terrestrial planets (abstract), *Lunar Planet. Sci. Conf., XXII*, 401-402, 1991.

Frey, H., Thermal history and climatic implications of early Hesperian ages for presumed Noachian age volcanic flows on Mars (abstract), *Lunar Planet. Sci. Conf., XXIII*, 385-386, 1992.

Golombek, M.P., Geometry of stresses around Tharsis on Mars (abstract), *Lunar Planet. Sci. Conf., XX*, 345-346, 1989.

Golombek, M.P., J. Suppe, W. Narr, J. Plescia and B. Banerdt, Does wrinkle ridge formation on Mars involve most of the lithosphere? (abstract), *Lunar Planet. Sci. Conf., XXI*, 421-422, 1990.

Golombek, M.P., J.B. Plescia and B.J. Franklin, Faulting and folding in the formation of planetary wrinkle ridges, *Proc. Lunar Planet Sci. Conf., 21st*, 679-693, 1991.

Greeley, R., and J.E. Guest, Geologic map of the eastern equatorial region of Mars, scale 1:15,000,000, *U.S. Geol. Surv. Misc. Invest. Ser. Map, I-1802-B*, 1987.

Greeley, R., and B.D. Schneid, Magma generation on Mars: Amounts, rates and comparisons with Earth, Moon, and Venus, *Science, 254*, 996-998, 1991.

Guth, P., Micronet: Interactive equal area and equal angle net, *Comput. Geosci., 13*, 541-543, 1987.

Hartman, W.K., et al., Chronology of planetary volcanism by comparative studies of planetary cratering, in *Basaltic Volcanism on the Terrestrial Planets*, pp. 1049-1127, Pergamon, New York, 1981.

Howard, K.A. and W.R. Muehlberger, Lunar thrust faults in the Taurus-Littrow region, *Apollo 17 Preliminary Science Report, NASA Spec. Publ., SP-330*, 31-22--31-25, 1973.

Janes, D.M., and H.J. Melosh, Tectonics of planetary loading: A general model and results, *J. Geophys. Res., 95*, 21,345-21,355, 1990.

Johnson, A.M., Folding and faulting of strain-hardening sedimentary rocks, *Tectonophysics, 62*, 251-278, 1980.

Kargel, J.S., and R.G. Strom, Ancient glaciation on Mars, *Geology, 20*, 3-7, 1992.

Lucchitta, B.K., Mare ridges and related highland scarps--Results of vertical tectonism, *Geochim. Cosmochim. Acta, 3, suppl.*, 2761-2782, 1976.

Lucchitta, B.K., Topography, structure, and mare ridges in southern Mare Imbrium and northern Oceanus Procellarum, *Geochim. Cosmochim. Acta, 3, suppl.*, 2691-2703, 1977.

Maxwell, T.A., F. El-Baz, and S.W. Ward, Distribution, morphology,and origin of ridges and arches in Mare Serenitatis, *Geol. Soc. Am. Bull., 86*, 1273-1278, 1975.

Maxwell, T.A. and R.J. Phillips, Stratigraphic correlation of the radar-detected subsurface interface in Mare Crisium, *Geophys. Res. Lett., 5*, 811-814, 1978.

Muehlberger, W.R., Structural history of southeastern Mare Serenitatis and adjacent highlands, *Geochim. Cosmochim. Acta, 1, suppl.*, 101-110, 1974.

Neukum G., and D.U. Wise, Mars: A standard crater curve and possible new time scale, *Science, 194*, 1381-1387, 1976.

Plescia, J.B. and M.P. Golombek, Origin of planetary wrinkle ridges based on the study of terrestrial analogs, *Geol. Soc. Am. Bull., 97*, 1289-1299, 1986.

Raitala, J.T., Highland wrinkle ridges on Mars (abstract), *Lunar Planet. Sci. Conf., XVIII*, 814-815, 1987.

Raitala, J.T., Superposed ridges on the Hesperia Planum area on Mars, *Earth Moon Planets, 40*, 71-99, 1988.

Schubert, G., and T. Spohn, Thermal history of Mars and the sulfur content of its core, *J. Geophys. Res., 95*, 14,095-14,104, 1990.

Schubert G., S.C. Solomon, D.L. Turcotte, M.J. Drake, and N.H. Sleep, Origin and thermal evolution of Mars, in *Mars*, edited by H.Kieffer, B. Jakosky, C. Snyder and M. Matthews, pp. 147-183, University of Arizona Press, Tucson, 1993.

Schultz, R.A., Assessment of global and regional teconic models for faulting in the ancient terrains of Mars, *J. Geophys. Res., 90*, 7849-7860, 1985.

Schultz, R.A., Strike-slip faulting of ridged plains near Valles Marineris, Mars, *Nature, 341*, 424-426, 1989.

Schultz, R.A., and K.L. Tanaka, Growth of the Coprates rise, Mars, as a result of lithospheric folding (abstract), *Lunar Planet. Sci. Conf., XXIII*, 1245-1246, 1992.

Scott D.H., and J.M. Dohm, Faults and ridges: Historical development in Tempe Terra and Ulysses Patera regions of Mars, *Proc. Lunar Planet. Sci. Conf., 20th*, 503-513, 1990.

Scott, D.H., and K.L. Tanaka, Geologic map of the western equatorial region of Mars, scale 1:15,000,000, *U.S. Geol. Surv. Misc. Invest. Ser. Map, I-1802-A*, 1986.

Sharpton, V.L., and J.W. Head, Stratigraphy and structural evolution of southern Mare Serenitatis: A reinterpretation based on Apollo Lunar Sounder Experiment data *J. Geophys. Res., 87*, 10,983-10,998, 1982.

Sharpton, V.L., and J.W. Head, Lunar mare ridges: Analysis of ridge-crater intersections and implications for the tectonic origin of mare ridges, *Proc. Lunar Planet. Sci. Conf., 18th*, 307-317, 1988.

Sleep, N.H., and R.J. Phillips, Gravity and lithospheric stress on the terrestrial planets with reference to the Tharsis region of Mars, *J. Geophys. Res., 90*, 4469-4489, 1985.

Solomon, S.C., and J.W. Head, Evolution of the Tharsis province of Mars: The importance of heterogeneous lithospheric thickness and volcanic construction, *J. Geophys. Res., 87*, 9755-9774, 1982.

Solomon, S.C., and J.W. Head, Heterogeneities in the thickness of the lithosphere of Mars: Constraints on heat flow and internal dynamics, *J. Geophys. Res., 95*, 1073-1083, 1990.

Stauffer, M.R., An empirical-statistical study of three-dimensional fabric diagrams as used in structural analysis, *Can. J. Earth Sci., 3*, 473-498, 1966.

Stevenson, D.J., and S.S. Bittker, Why existing terrestrial planet thermal history calculations should not be believed (and what to do about it)(abstract), *Lunar Planet. Sci. Conf., XX*, 515-516, 1990.

Strom, R.G., N.J. Trask, and J.E. Guest, Tectonism and volcanism on Mercury, *J. Geophys. Res., 80*, 2478-2507, 1975.

Tanaka, K.L., The stratigraphy of Mars, *Proc. Lunar Planet. Sci. Conf. 17th, Part 1, J. Geophys. Res., suppl.*, E139-158, 1986.

Tanaka, K.L., and D.H. Scott, Geologic maps of the polar regions of Mars, scale 1:15,000,000, *U.S. Geol. Surv. Misc. Invest. Ser. Map, I-1802-C*, 1987.

Tanaka, K.L., N.K. Isbell, D.H. Scott, R. Greeley and J.E. Guest, The resurfacing history of Mars: A synthesis of digitized, Viking-based geology, *Proc. Lunar Planet. Sci. Conf., 18th*, 665-678, 1988.

Tanaka, K.L., M.P. Golomoek, and W.B. Banerdt, Reconciliation of stress and structural histories of the Tharsis region of Mars, *J. Geophys. Res., 96*, 15,617-15,633, 1991.

Turcotte, D.L. and G. Schubert, *Geodynamics: Application of Continuum Physics to Geological Problems*, p. 450, John Wiley, New York, 1982.

Watters, T.R., Thin and thick-skinned deformation in the Tharsis region of Mars (abstract), Reports of Planetary Geology Program 1986, *NASA Tech. Memo., TM89801*, 481-483, 1987.

Watters, T.R., Wrinkle ridge assemblages on the terrestrial planets, *J. Geophys. Res., 93*, 10,236-10,254, 1988.

Watters, T.R., Origin of periodically spaced wrinkle ridges on the Tharsis plateau of Mars, *J. Geophys. Res., 96*, 15,599-15,616, 1991.

Watters, T.R., A system of tectonic features common to Earth, Mars and Venus, *Geology, 20*, 609-612, 1992.

Watters, T.R., and D.J. Chadwick, Crosscutting periodically spaced first-order ridges in the ridged plains of Hesperia Planum: Another case for a buckling model (abstract), in *MEVTV Workshop on Tectonic Features on Mars*, edited by T.R. Watters and M.P. Golombek, pp. 36-38, Lunar and Planetary Institute, Houston, Tex., 1989.

Watters, T.R., and R.A. Craddock, Nature and origin of wrinkle ridges in the floor material of Kasei Valles, Mars (abstract), *Lunar Planet Sci. Conf., XXII*, 1475-1476, 1991.

Watters, T.R. and T.A. Maxwell, Crosscutting relations and relative ages of ridges and faults in the Tharsis region of Mars, *Icarus, 56*, 278-298, 1983.

Watters, T.R., and T.A. Maxwell, Orientation, relative age, and extent of the Tharsis Plateau ridge system, *J. Geophys. Res., 91*, 8113-8125, 1986.

Watters, T.R., M.J. Tuttle and J. Chadwick, Mare ridge-Highland scarp structures and upland scarps on the Moon, Mars and Mercury (abstract), *Lunar Planet. Sci. Proc., XIX*, 1247-1248, 1988.

Watters, T.R., M.J. Tuttle, and F.J. Kiger, Symmetry of inferred stress fields in the Tharsis region of Mars (abstract), *Lunar Planet Sci. Conf., XXI*, 1312-1313, 1990.

Watters, T.R., M.J. Tuttle, and D. Simpson, Wrinkle ridge-upland scarp transitions: Implications for the mechanical properties of the deformed materials (abstract), *Lunar Planet. Sci. Conf., XXII*, 1477-1478, 1991.

Wilhelms, D.E., and R.J. Baldwin, The role of igneous sills in shaping the Martian uplands, *Proc. Lunar Planet. Sci. Conf., 19th*, 355-365, 1989.

Willemann, R.J., and D.L. Turcotte, The role of lithospheric stress in the support of the Tharsis rise, *J. Geophys. Res., 87*, 9793-9801, 1982.

Wise, D.U., Golombek, M.P., and G.E. McGill, Tharsis province of Mars: Geologic sequence, geometry and a deformation mechanism, *Icarus, 38*, 456-472, 1979.

Zimbelman, J.R., Solomon, S.C., and V.L. Sharpton, The evolution of volcanism, tectonics and volatiles on Mars: An overview of recent progress, *Proc. Lunar Planet. Sci., 21st*, 613-626, 1991.

Zuber, M.T., and L.L. Aist, The shallow structure of the Martian lithosphere in the vicinity of the ridged plains, *J. Geophys. Res., 95*, 14,215-14,230, 1990.

Zuber, M.T., D.E. Smith, S.C. Solomon, D.O. Muhleman, J.W. Head, J.B. Garvin, J.B. Abshire, and J.L. Bufton, The Mars Observer Laser Altimeter investigation, *J. Geophys. Res., 97*, 7781-7797, 1992.

T.R. Watters, Center for Earth and Planetary Studies, National Air and Space Museum, Smithsonian Institution, Washington, DC 20560.

(Received September 4, 1992;
revised April 14, 1993;
accepted April 26, 1993.)